Radiocarbon, Vol 00, Nr 00, 2023, p 1–12 DOI:10.1017/RDC.2023.109
Selected Papers from the 24th Radiocarbon and 10th Radiocarbon & Archaeology International Conferences, Zurich, Switzerland, 11–16 Sept. 2022

PREPARATION AND HANDLING OF METHANE FOR RADIOCARBON ANALYSIS AT COLOGNEAMS

Jan Olaf Melchert[1]* • Martina Gwozdz[2] • Merle Gierga[1] • Lukas Wacker[3] • Dennis Mücher[2] • Janet Rethemeyer[1]

[1]Institute for Geology and Mineralogy, University of Cologne, Cologne, Germany
[2]Institute for Nuclear Physics, University of Cologne, Cologne, Germany
[3]Laboratory of Ion Beam Physics, ETH, Zürich, Switzerland

ABSTRACT. CH_4 is the second most important anthropogenic greenhouse gas and originates from different sources. The use of radiocarbon (^{14}C) analysis of CH_4 opens up the possibility to differentiate geological and agricultural origin. At the CologneAMS facility, the demand for ^{14}C analysis of CH_4 required the development of a sample handling routine and a vacuum system that converts CH_4 to CO_2 for direct injection of CO_2 into the AMS. We evaluated the processing of CH_4 using several series of gas mixtures of ^{14}C-free and modern standards as well as biogas with sample sizes ranging from 10 to 50 µg C. The results revealed a CH_4 to CO_2 conversion efficiency of 94–97% and blank values comparable to blank values achieved with our routinely used vacuum system for processing CO_2 samples. The tests with a near modern CH_4:CO_2 biogas mixture gave reproducible results with a near modern ^{14}C content of 0.967–1.000 $F^{14}C$, after applying the background correction.

KEYWORDS: AMS, gas ion source, methane, radiocarbon, small-scale radiocarbon analysis.

INTRODUCTION

The global atmospheric methane (CH_4) concentration has more than doubled since the 19th century and is increasing even more rapidly since 2007 (Saunois et al. 2020). After carbon dioxide (CO_2), CH_4 is considered to be the second most important greenhouse gas with a 28–36 times larger greenhouse gas warming potential compared to CO_2. When looking at its impact over 100 years, 1 tonne of CH_4 is equivalent to 28–36 tonnes of CO_2 (IPCC AR5; Myhre et al. 2013.). Therefore, CH_4 is more powerful at trapping heat in the atmosphere than CO_2 on a per molecule basis and thus has an important influence on the rate of climate change (Saunois et al. 2016).

CH_4 in the atmosphere originates from many different sources, which are difficult to identify and quantify. Presently, the dominant global sources of anthropogenic CH_4 emissions are agriculture, fossil fuel production and combustion (Kirschke et al. 2013; Turner et al. 2017; Maasakkers et al. 2019). While agricultural CH_4 emissions derive mainly from ruminant animals, organic matter degradation through methanogens is responsible for wetland CH_4 emissions. Whereas the extraction, storage, and transportation of oil, natural gas, and coal release CH_4 generated by thermogenic (geological) processes. These CH_4 sources have characteristic ^{13}C and ^{14}C isotopic signatures. CH_4 produced by methanogenesis of fresh organic matter is depleted in its ^{13}C content and enriched in ^{14}C, whereas thermogenic degradation of organic matter in sedimentary rocks generates CH_4 that contains more ^{13}C compared to biogenic sources and no ^{14}C.

To distinguish between C sources, numerous studies have applied carbon isotopic analysis of CH_4 emissions over the last years. While many of these investigations use ^{13}C analysis (Lowry et al. 2001; Fisher et al. 2011; Townsend-Small et al. 2016; Lopez et al. 2017; Maazallahi et al. 2020),

*Corresponding author. Email: jan.melchert@uni-koeln.de

other studies applied ^{14}C analysis to distinguish CH_4 sources in the atmosphere (Graven et al. 2019; Zazzeri et al. 2021), in peatland (Garnett et al. 2016; Cooper et al. 2017) or in aquatic systems (Pohlman et al. 2009; Joung et al. 2019) or the combination of both isotopes has been applied (Gonzalez Moguel et al. 2022).

Unfortunately, in contrast to ^{13}C, the direct ^{14}C analysis of CH_4 is not possible and requires an elaborate pre-treatment routine during which the CH_4 is purified and subsequently oxidized to CO_2 for further analysis. Gas samples taken from the environment or from laboratory incubations contain other C carrying gases that need to be separated from CH_4 by utilizing carrier gases (noble gas or synthetic air, Pohlman et al. 2009) or pressure differences (Garnett et al. 2019) by which the sample is moved through chemical adsorbents (Garnett et al. 2019; Zazzeri et al. 2021; Gonzalez Moguel et al. 2022) and cryogenic traps (Petrenko et al. 2008; Pack et al. 2015) or a combination of those (Garnett et al. 2019; Gonzalez Moguel et al. 2022). The approach presented in this study utilizes a combination of methods taken from recent studies including a set of cryogenic traps, an oxidation furnace and synthetic air as carrier gas operating below ambient pressure.

Environmental gas samples most prominently contain CO_2 and water (H_2O) but also carbon monoxide (CO) and other hydrocarbon gases in smaller quantities. As these gases are potentially emitted from different organic or inorganic sources having different isotopic compositions, it is necessary to eliminate them (Petrenko et al. 2008). H_2O is removed using dry ice slurries (DI) or adsorbents (Garnett et al. 2019; Zazzeri et al. 2021), while CO_2 is trapped in liquid nitrogen (LN; Petrenko et al. 2008; Pack et al. 2015) or adsorbed through molecular sieves containing zeolite (Garnett et al. 2019; Zazzeri et al. 2021). Depending on the origin and composition of the gas sample, the removal of CO may be essential because it is oxidized in the furnace along with the CH_4, which may bias the result of the CH_4 (Pack et al. 2015). Ultimately, the purified CH_4 is oxidized in a furnace with an oxygen donor and converted to CO_2 and H_2O. The choice of the catalyst varies from laboratory to laboratory. Most prominently, cupric oxide (CuO) filled columns (Kessler and Reeburgh 2005; Pack et al. 2015), platinized alumina beads contained in quartz glass tubes (Garnett et al. 2019; Gonzalez Moguel et al. 2022) or platinized quartz wool are used as catalysts (Petrenko et al. 2008; Sparrow and Kessler 2017; Zazzeri et al. 2021). After the reaction, the CH_4-derived CO_2 can be quantified and prepared for ^{14}C analysis via gas injection or graphitization, i.e., conversion to elemental C.

Here we present a flow-through vacuum system coupled with cryogenic traps for the purification and conversion of CH_4 samples to CO_2 for the purpose of radiocarbon analysis at the CologneAMS facility. The system operates at low pressures (30 mbar) and is by design applicable for the processing of gaseous samples of different origin via syringes or capillaries that can be attached to the system. The system can handle large and small samples, but it was mainly designed for 15–50 µg C, that is the typical sample size for CO_2 analysis using the gas ion source of our AMS at Cologne University.

METHODS

System Overview

The CH_4 oxidation system consists of (1) the mixing unit, where samples or standard gas mixtures are prepared and injected via the gas supplies, (2) the CH_4 purification unit consisting of furnaces and cryotraps, and (3) the sealing unit where the sample can be quantified and CO_2 aliquots corresponding to 10–50 µg C are sealed off for subsequent AMS measurement (Figure 1).

https://doi.org/10.1017/RDC.2023.109 Published online by Cambridge University Press

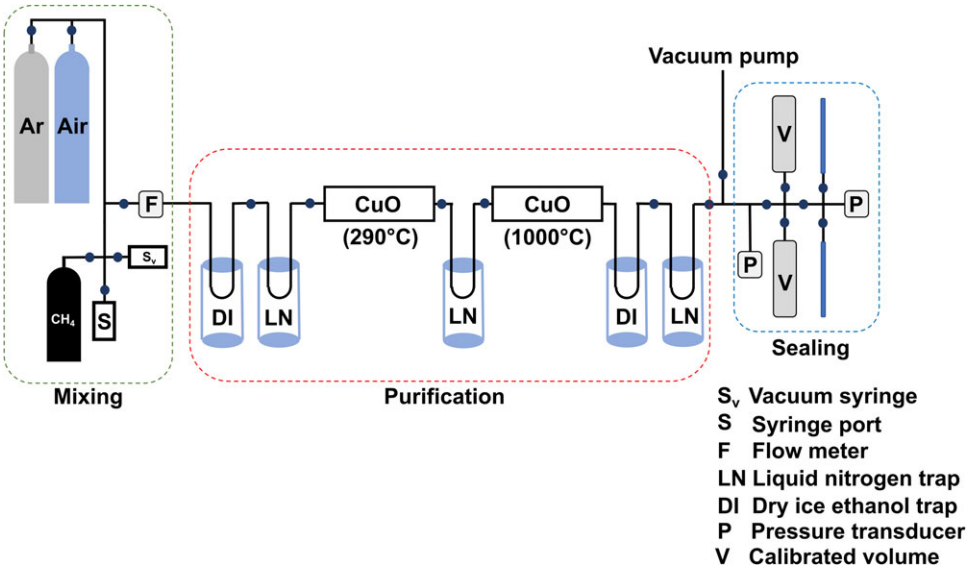

Figure 1 Schematic overview of the oxidation rig consisting of the mixing (green), purification (red) and sealing (blue) units. (Please see online version for color figures.)

In the mixing unit, each connection is individually maintainable by a respective valve allowing the injection and mixing of defined volumes of gas mixtures. CH_4 and CO_2 are supplied either in pressurized 15 L bottles that are directly connected to the mixing unit with a pressure regulator and regular ferrule fittings (Swagelok®, USA), from a self-assembled stainless-steel cylinder (304L-HDF4-1GAL, Swagelok®, USA) that is equipped with a pressure gauge (-1 – 3 bar, PGI-63B-BC3-LAQX, Swagelok®, USA) and a septum port (SS-4-TA-1-4STKZ, Swagelok®, USA) or the gases are taken from sealed serum bottles. Similar to the sample cylinder, a septum port (S, Figure 1) is used for syringe injection of gases with a 10 mL gas tight syringe (Gastight 1010 LTN, Hamilton®, USA). In addition, a 2.5 mL stainless-steel vacuum syringe (S_V, Figure 1, KDScientific Inc., USA) with a screw thread for standard vacuum fittings was installed in order to mix bottled gas with gases injected with a syringe. The valves are permanently regulating the gas flow so that a gas stream of 60 mL min^{-1} cannot be exceeded. The flow is monitored by a flow meter (F, Figure 1, FMA-1606, Omega™ Engineering Inc., USA) that is installed prior to the purification unit of the oxidation rig.

Gases are flushed from the mixing unit through a U-tube submerged in a Dewar flask filled with dry ice (DI) trapping moisture, while a second U-tube in a Dewar flask filled with liquid nitrogen (LN) traps CO_2 from the gas stream. After removal of moisture and CO_2, the gas flows through a furnace via a CuO-filled quartz glass tube that is heated to 290°C. Thereby CO is removed from the gas phase and oxidized to CO_2, which is then trapped in another LN trap installed behind the furnace. Subsequently, the gas stream enters a second furnace (Carbolite Gero GmbH & Co. KG) with a CuO-filled quartz glass tube that is heated at 1000°C in order to oxidize CH_4 to CO_2 (red frame, Figure 1). In a final set of cryogenic traps, H_2O and CO_2 are collected within U-tubes submerged in DI and LN, respectively. Any non-reactive and non-condensable gases left in the gas stream are now evacuated through the vacuum pump and the isolated CO_2 is transferred to the sealing unit.

https://doi.org/10.1017/RDC.2023.109 Published online by Cambridge University Press

The sealing unit (blue frame, Figure 1) is constructed like a standard vacuum rig with pressure transducers, calibrated volumes, and ultra-torr fittings equipped with glass ampoules (4 or 6 mm OD), that are used to seal CO_2 samples (Wotte et al. 2017). The sample CO_2 is first trapped in a LN-filled Dewar flask and then transferred into a calibrated volume for quantification. Defined amounts of CO_2 can be transferred via a second calibrated volume into glass ampoules with the help of LN. Non-condensable gases are removed by briefly opening the valves (V) prior to sealing the ampoules with a hand-torch.

Sample Preparation

Prior to sample processing, the tube furnace is heated up to 1000°C for 30 min to ensure temperature equilibration. The mixing and purification units of the system are flushed three times with argon (Ar) for 5 min (40 mL min^{-1}) and evacuated afterwards below 10^{-3} mbar. This is also done between samples to maintain a low line blank and prevent memory effects (Pack et al. 2015). The synthetic air is set to a flow rate of 10 mL min^{-1} during the entire sample preparation procedure. The pressure in the system is < 20 mbar throughout the sample processing, which still ensures the removal of other hydrocarbon gases from the gas phase into the LN trap and, more importantly, prevents the condensation of oxygen, which might pose a safety hazard (Sparrow and Kessler 2017). The sealing part of the system is not flushed and kept at a constant vacuum below 10^{-7} mbar to maintain cleanliness.

Depending on the type of sample or standard, different injection and mixing procedures are possible at the mixing unit of the oxidation rig that will be addressed individually in more detail below. Injected gas mixtures are transported via the synthetic air stream through the furnaces and cryogenic traps in the purification unit into the calibrated volumes and glass ampoules at the sealing unit.

Preparation of Standards

Carbon Free Standards

Different types of standards were prepared to test the overall cleanliness of the setup as well as of the trapping efficiency and the CH_4 to CO_2 conversion rate of the oxidation rig. The overall C blank of the line was tested by C-free N_2 gas with the system (99.999% purity, Linde GmbH, Germany). The N_2 was filled via a Teflon tube attached to sterile injection needles (Sterican® size 18, B. Braun SE, Germany) into 100 mL serum bottles sealed with crimped butyl rubber stoppers. Ambient air was released from the bottle via a second injection needle. The serum bottles were previously washed with Milli-Q water (MQ; Millipore, USA), combusted at 450°C for 3 hr and flushed at ambient pressure with N_2 with at least three bottle volumes to ensure that no ambient air remained inside. A 10 mL gas tight syringe, which was pre-cleaned with dichloromethane (DCM; SupraSolv®, MERCK KGaA, Germany) to remove residual lubricants, was used to extract 10 mL N_2 from the sealed serum bottle and inject the gas into the oxidation rig via the septum port (S, Figure 1).

Efficiency of CO Removal

The efficiency of CO removal was tested using a N_2/CO mixture (CO concentration 100 ppm, 12 L ALLCAN, All-in-Gas E.K., Munich, Germany). Due to safety measures, we were not able to handle pure bottled CO. Several pre-washed 100 mL serum bottles sealed with butyl rubber stoppers were flushed at about ambient pressure with this gas mixture via injection needles. A Teflon tube with injection needles on both ends was then used to transfer the N_2/CO

https://doi.org/10.1017/RDC.2023.109 Published online by Cambridge University Press

mixture via the septum port into the oxidation rig. The flowrate was increased from 60 mL/min to 120 mL/min during each injection, while the furnace was heated at 250°C and, in another series, at 290°C, comparable to Pack et al. (2015). The gas mixture was flushed from the serum bottles into the vacuum system.

Modern Standards

^{14}C-enriched CO_2 standards (Ox-II; NIST SRM 4990C; nominal value 1.3407 $F^{14}C$) were prepared with sealed tube combustion of oxalic acid crystals according to Melchert et al. (2019). In summary, oxalic acid powder equal to 3 mg of C was weighed into DCM-cleaned Sn boats (4 × 4 × 11 mm, Elementar, Germany) and transferred into quartz tubes (MQ-washed and pre-combusted at 900°C) along with CuO as a combustion catalyst. The quartz tubes were evacuated at a vacuum rig below 10^{-3} mbar and sealed using a blow torch and combusted at 900°C for 4 hr. After combustion, the cool tubes were wiped with acetone (PESTINORM® SUPRA TRACE, grade ≥99.9%, VWR® chemicals, Germany), to remove potential dust and cloth fibres from the surface and put in a tube cracker at the vacuum rig. The CO_2 was flushed with a He stream through a dry-ice ethanol slurry to remove any excess moisture and then through a LN-filled cryotrap to fixate the CO_2. Subsequently, the amount of CO_2 was quantified and sealed off in a glass ampoule that was carefully inserted inside a 100 mL serum bottle sealed with a butyl stopper and flushed with He for 10 min (40 mL min^{-1}) via injection needles at ambient pressure. After flushing, the serum bottle was thoroughly shaken to break the glass ampoule inside in order to release the CO_2. Lastly, a 10 mL aliquot of the CO_2:He mixture was extracted using the gas tight syringe and injected into the oxidation rig via the syringe port.

Fossil Standards

Two mL of bottled ^{14}C-free CH_4 (99.995% purity, Westfalen AG, Germany) were injected at ambient pressure as a ^{14}C-free standard and, in a second series, mixed with ^{14}C-enriched CO_2 from oxalic acid. With this second series, we tested the efficiency to trap CO_2 that does not originate from CH_4 and separate it from CH_4-derived CO_2. A ratio of 2 mL CH_4 to 10 mL of He:CO_2 gas mixture was injected to provide a sensitive measure for the separation of ^{14}C-free CO_2 derived from CH_4 and ^{14}C-enriched CO_2 originated from Ox-II. Therefore, the synthetic air stream was closed and the mixing unit was evacuated. Then, the CH_4 bottle was opened and set up at 1 bar to fill the 2 mL vacuum syringe. The valves next to the vacuum syringe and the CH_4 supply were then closed and the system left to evacuate. Subsequently, the synthetic air stream was opened again and set up at 10 mL min^{-1}. Up to this point, no cryogenic traps were yet attached and the residual CH_4 was pumped out of the system. 10 mL aliquots of the Ox-II derived CO_2:He mixture were extracted from the 100 mL serum bottles using the gas tight syringe and inserted into the septum port. The DI ethanol slurry and LN traps were attached to the U-tubes, the valves to the line were opened and the gases were flushed through the setup via the stream of synthetic air. After the injection, the valves to the septum port and vacuum syringe were closed and the system was flushed for 10 min with synthetic air to ensure that the gas mixture was moved completely through the setup.

Biogas Mixture

Biogas collected from a nearby biogas facility (RheinEnergie Biogasanlage Randkanal-Nord, Dormagen, Germany) in a pre-evacuated stainless-steel cylinder was used as a near-modern CH_4 laboratory standard. At the biogas facility, the cylinder was directly connected to one of the maintenance gas outlets via a Teflon coated tube. The valves were opened after connecting the tube to flush the cylinder for about 5 min. The biogas mainly consists of CH_4 and CO_2

https://doi.org/10.1017/RDC.2023.109 Published online by Cambridge University Press

Table 1 Comparison of different standard series handled on the CH_4 oxidation rig, expected and measured $F^{14}C$ (average value with standard deviation), as well as recovery efficiency.

Sample	n	Expected $F^{14}C_R$	Measured $F^{14}C_S \pm 1\sigma$	Efficiency (%)
CH_4:CO_2 (dead:Ox-II)	13	0	0.006 ± 0.006	94.4
CH_4:CO_2 (biogas)	9	~1	0.983 ± 0.016	97.3
CH_4 (dead)	11	0	0.003 ± 0.003	—
CO_2 (Ox-II)	7	1.341	1.346 ± 0.015	—

among other trace gases (56% CH_4, 44% CO_2, quantified by the supplier). 10 mL aliquots were extracted from the cylinder at ambient pressure by connecting a second valve with septum port to the cylinder and using the gas tight syringe and immediately injected into the oxidation rig, similar to the procedure for the previously described Ox-II CO_2 standards.

The ^{14}C results for the biogas were background corrected using the average ^{14}C concentration from the injection of pure ^{14}C-free CH_4 (0.003 ± 0.003 $F^{14}C$, Table 1).

RESULTS AND DISCUSSION

In order to test our oxidation system for recovery efficiency and contamination, a total of 40 aliquots from multiple 2 mL and 10 mL injections containing between 10 and 50 µg C were processed for AMS analysis. The results of the different series are summarized in Figure 2 and Table 1, and the raw AMS results are summarized in the supplementary material (Table S1).

^{14}C Analysis of Standards

CO_2 produced from pure ^{14}C-free CH_4 had an average $F^{14}C$ of 0.003 ± 0.003 (n = 11). The same CH_4 that was mixed with Ox-II derived CO_2 contained slightly more ^{14}C (0.006 ± 0.006 $F^{14}C$; n = 13). The blank values obtained from these series are comparable to blank standards of a similar size prepared on our CO_2 vacuum line that is used for small samples (10–50 µg C) including compound-specific radiocarbon analysis ($F^{14}C$ 0.005 ± 0.0004; n = 4; Melchert et al. 2019). However, the blank values shown here are up to one order of magnitude higher compared to other studies (Table 2), which we think is most likely related to the much smaller size of our samples. In contrast to other studies, the CO_2 is processed for direct injection into the AMS, instead of graphitization and AMS analysis as solid target, making the samples more sensitive to contributions by extraneous C. The ^{14}C content of pure CO_2 produced from Ox-II (n = 7) is close to that of the consensus value with a $F^{14}C$ of 1.346 ± 0.015, while the injection of carbon-free N_2 gas gave no quantifiable amount of C via AMS analysis. This indicates that the system operates without quantifiable leakages. The results of the analysis of ^{14}C-enriched CO_2, ^{14}C-free CH_4 and C-free N_2 further indicate that the sample handling, which includes the sealing of gas in serum bottles and transfer of aliquots via syringes, does not introduce substantial amounts of contamination.

Estimating Extraneous Carbon

The amount of extraneous C introduced during sample processing was determined from the ^{14}C data of standard CH_4, which was on average 0.20 ± 0.23 µg modern C. This amount of

https://doi.org/10.1017/RDC.2023.109 Published online by Cambridge University Press

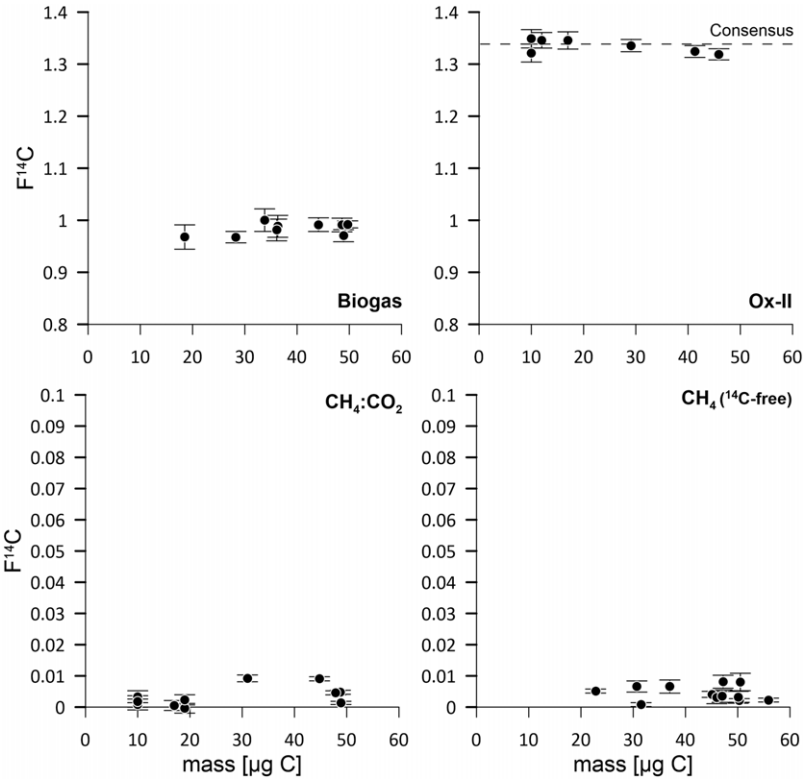

Figure 2 Results of AMS ^{14}C measurements for the biogas mixture, of modern and ^{14}C-free standards as well as of the CH_4:CO_2 gas mixture (^{14}C-free:^{14}C-enriched).

modern contamination is similar to values reported by Pack et al. (2015) and Sparrow and Kessler (2017). The ^{14}C data of the ^{14}C-enriched standards were expected to show a size dependency, i.e., an increase in F^{14}C with decreasing sample size and vice versa, following the concept of the introduction of a constant amount of contamination (Ruff et al. 2010; Rethemeyer et al. 2013; Melchert et al. 2019). Only weak to moderate correlation coefficients after Pearson could be determined for the distribution of F^{14}C versus sample size for the injected series of samples (^{14}C-free CH_4 $r = 0.5$; ^{14}C-free CH_4:Ox-II CO_2 $r = 0.1$; Ox-II CO_2 $r = -0.64$; biogas $r = 0.46$). The results of the Ox-II standards summarized in Figure 2 and the negative correlation coefficient, do not show an assessable pool of fossil contamination, although, the standards were sealed in serum bottles closed with butyl rubber stoppers, which have been shown to introduce fossil CO_2 by outgassing (Gao et al. 2014; Pack et al. 2015). This could either indicate, that during the extra steps of oxalic acid handling (sealed tube combustion, sealing in ampoules, storing in serum bottles) no more additional contaminant has been added or that the size of the standards (10 mL Ox-II:He mixture) is too large to identify additional contamination. Because of this, the thorough assessment of extraneous C via a model of constant contamination is not supported by the data distribution. Furthermore, pure N_2 gas from sealed serum bottles contained no C, which either indicates that the outgassing of butyl only happens after longer storage or is below detection limit of the pressure transducers at the oxidation system.

https://doi.org/10.1017/RDC.2023.109 Published online by Cambridge University Press

Table 2 Overview over blank values of this and other studies as well as measured (S) and contamination corrected (R) ^{14}C data for biogas (own data are mean values with propagated errors) as well as amounts of contaminants (m_{modern}; m_{dead}).

Author	$F^{14}C_{dead}$ CH_4	m_{modern} [µg C]	$F^{14}C_{modern+dead}$	$m_{modern+dead}$ [µg C]	m_S [µg C]
^{14}C-free standard					
This study	0.003 ± 0.003	0.2 ± 0.2	—	—	10–50[a]
Pack et al. (2015)	0.0016 ± 0.0003	0.4 ± 0.2	—	—	>500[b]
Garnett et al. (2019)	0.0011 – 0.0016	1.9 – 3.8	—	—	>500[b]
Palonen et al. (2017)	0.0006 ± 0.0007*[1]	—	—	—	1000[b]
Petrenko et al. (2008)	0.0022 ± 0.0004	—	0.236 ± 0.162	0.23 ± 0.16	130–190[b]
Sparrow and Kessler (2017)	0.0023 ± 0.0007	0.24	—	—	451–839[b]
Biogas					
Author	$F^{14}C_S$		$F^{14}C_R$		m_S (µg C)
This study	0.967–1.000		0.967–1.000*[2]		20–50[a]
Garnett et al. (2019)	—		0.978–0.987*[3]		>500[b]
Palonen et al. (2017)	—		1.045 ± 0.005*[1]		1000[b]

*[1]Background corrected for 0.004 ± 0.001 $F^{14}C$
*[2]background corrected for 0.003 ± 0.003 $F^{14}C$
*[3]background corrected for 0.0017 $F^{14}C$
[a]AMS measurement of CO_2
[b]AMS measurement of graphite.

^{14}C Analysis of Biogas

Near modern biogas was collected at a nearby biogas facility and used as a nearly modern in-house CH_4 standard. Buyable CH_4 gas is mostly produced from natural gas and oil residues and is therefore ^{14}C-depleted. The sizes of the biogas samples ranged from 20 to 50 µg C (n = 9) and gave ^{14}C contents in a narrow range of 0.967 to 1.000 $F^{14}C$ (Table 2). We observed a small decrease in $F^{14}C$ with decreasing sample size. The ^{14}C data of processed blank standards were used for the correction of the biogas data, which did not significantly increase ^{14}C contents of the biogas. Because the presented data are the first tests with biogas of this facility, we have no distinct reference values like other authors (Palonen et al. 2017; Garnett et al. 2019).

CH_4 Oxidation Efficiency and Recovery

For several injection series, an average of about 94.4% of ^{14}C-free CH_4 from the CH_4:CO_2 gas mixture was oxidized to CO_2. An even higher amount of 97.3% CH_4-derived CO_2 was recovered after the oxidation of the CH_4:CO_2 gas mixture. The ^{14}C content of the CH_4:CO_2 gas mixture was similar to the ^{14}C content of the pure CH_4 standards underlining the efficient separation of CO_2 from CH_4.

A temporary installation of a second LN trap behind the oxidation furnace (not included in Figure 1), as suggested by various authors (Petrenko et al. 2008; Pack et al. 2015; Sparrow and Kessler 2017), did not increase the recovery efficiency, from which we deduced that our traps work sufficiently. The oxidation efficiency and calculated recoveries may be slightly biased by small losses of sample material related to the manual sample extraction and injection with the syringe that was not specifically accounted for. Furthermore, the oxidation efficiency and recovery are likely linked to the type of catalyst and to the packing and compaction of the catalyst inside the oxidation tube (Sparrow and Kessler 2017). We decided to use CuO rods, because they are easy to handle, cost efficient and are already routinely used in our laboratory. Pack et al. (2015) reported a very high oxidation efficiency of about 100% with CuO, while Sparrow and Kessler (2017) used platinized quartz wool to achieve consistently high efficiencies. The CuO is rather loosely packed in the quartz tube over almost the entire length of about 30 cm and fixated on each side with quartz wool, which should allow the gas to heat up properly and react with the catalyst without restricting gas flow.

The injection of pure CO_2 at different flow rates of synthetic air up to 80 mL min^{-1} gave no changes in the amount of CO_2 trapped with LN as observed by Pack et al. (2015), who installed an additional CO_2 trap to improve recoveries. Achieved flow rates and the pressure inside the system are highly dependent on the scale of the setup, i.e., length and diameter of the capillaries and components. Therefore, advice given on optimal setup conditions are, unfortunately, not universally applicable.

CO Oxidation Efficiency

Multiple injections of N_2/CO mixtures (100 ppm CO) from sealed 100 mL serum bottles indicated an oxidation efficiency of CO to CO_2 of 98–99% at 290°C (n = 5). Variations of the flow rate from 60 mL/min up to 120 mL/min neither influenced oxidation nor trapping efficiency. However, decreasing the temperature of the CO furnace to 250°C significantly decreased the oxidation efficiency to 12.5 % (n = 3). From this finding we conclude that the efficiency of the setup is dependent on the furnace temperature and not on the flow rate, which

https://doi.org/10.1017/RDC.2023.109 Published online by Cambridge University Press

was similarly concluded by Pack et al. (2015), although a stable oxidation rate was reported there for 250°C using the same catalyst (CuO).

Limitation of Sample Sizes

In this manuscript we only evaluated small volume samples containing higher CH_4 concentrations than natural samples. From these high concentration samples, we deduced that neither the combustion furnaces, nor our cryogenic traps were overloaded. Thus, samples that are less concentrated in CH_4, for example atmospheric samples that on average contain 2 ppm CH_4 and are sampled in bags exceeding 100 L (Townsend-Small et al. 2012; Espic et al. 2019), should not overload the traps either. However, their processing will take much longer using the flow rates established in this study. This practically excludes the processing of very low concentration samples (i.e., atmospheric) because it would take multiple hours to fully inject such a sample into the system. Thus, the presented system is suitable for the processing of gases from laboratory incubation experiments as well as natural wetland emissions provided from canisters or gas bags.

CONCLUSION

The need for radiocarbon dating of CH_4 required the development of methods and systems for processing such samples at the CologneAMS dating center. The constructed vacuum system, which converts CH_4 to CO_2 for direct injection of CO_2 into the AMS, was tested with ^{14}C-free and modern standards and a near modern biogas. Sample sizes measured with the gas ion source were all in the range of 10 and 50 µg C. The results of these tests reveal the quantifiable contribution of about 0.20 ± 0.23 µg modern extraneous carbon that is introduced during sample handling. The collection and analysis of a CH_4:CO_2 biogas mixture representing a "natural" gas gave reproducible results (0.967–1.000 $F^{14}C$). The conversion rate of CH_4 to CO_2 that was calculated from the analyses of standards and biogas was about 94–97% and may be further improved in the future by changing the types and packing of the oxidation catalyst inside the furnace as shown in previous studies. In summary, the preparation and handling of CH_4 derived CO_2 for AMS analysis is operational at CologneAMS. The current pre-treatment methods and handling of suitable samples within 1 h is time efficient and the usage of CuO catalysts and cryogenic traps instead of chemicals is cost efficient.

SUPPLEMENTARY MATERIAL

To view supplementary material for this article, please visit https://doi.org/10.1017/RDC.2023.109

ACKNOWLEDGMENTS

We thank Marcus Brand from Rheinenergie for the possibility of visiting the biogas facility Randkanal Nord and the opportunity to sample gas directly from the facility.

PREVIOUS PUBLICATION

An early version of this manuscript was used as part of a doctoral dissertation and had to be published in the online repository at University of Cologne (http://kups.ub.uni-koeln.de/id/eprint/55058). The publication of this early manuscript iteration was done for academic purposes only.

REFERENCES

Cooper MDA, Estop-Aragonés C, Fisher JP, Thierry A, Garnett MH, Charman DJ, et al. 2017. Limited contribution of permafrost carbon to methane release from thawing peatlands. Nat. Clim. Change 7:507–511. doi: 10.1038/nclimate3328

Espic C, Liechti M, Battaglia M, Paul D, Röckmann T, Szidat S. 2019. Compound-specific radiocarbon analysis of atmospheric methane: a new preconcentration and purification setup. Radiocarbon 61(5):1461–76. doi: 10.1017/RDC.2019.76

Fisher RE, Sriskantharajah S, Lowry D, Lanoisellé M, Fowler CMR, James RH, et al. 2011. Arctic methane sources: Isotopic evidence for atmospheric inputs. Geophys. Res. Lett. 38. doi: 10.1029/2011GL049319

Gao P, Xu X, Zhou L, Pack MA, Griffin S, Santos GM, et al. 2014. Rapid sample preparation of dissolved inorganic carbon in natural waters using a headspace-extraction approach for radiocarbon analysis by accelerator mass spectrometry. Limnol. Oceanogr. Methods 12:174–190. doi: 10.4319/lom.2014.12.174

Garnett MH, Gulliver P, Billett MF. 2016. A rapid method to collect methane from peatland streams for radiocarbon analysis. Ecohydrology 9: 113–121. doi: 10.1002/eco.1617

Garnett MH, Murray C, Gulliver P, Ascough PL. 2019. Radiocarbon analysis of methane at the NERC Radiocarbon Facility (East Kilbride). Radiocarbon 61:1477–1487. doi: 10.1017/RDC.2019.3

Gonzalez Moguel R, Vogel, F, Ars S, Schaefer H, Turnbull JC, Douglas PMJ. 2022. Using carbon-14 and carbon-13 measurements for source attribution of atmospheric methane in the Athabasca oil sands region. Atmospheric Chem. Phys. 22:2121–2133. doi: 10.5194/acp-22-2121-2022

Graven H, Hocking T, Zazzeri G. 2019. Detection of fossil and biogenic methane at regional scales using atmospheric radiocarbon. Earths Future 7:283–299. doi: 10.1029/2018EF001064

Joung D, Leonte M, Kessler JD. 2019. Methane sources in the waters of Lake Michigan and Lake Superior as revealed by natural radiocarbon measurements. Geophys. Res. Lett. 46, 5436–5444. doi: 10.1029/2019GL082531

Kessler JD, Reeburgh WS. 2005. Preparation of natural methane samples for stable isotope and radiocarbon analysis: Methane isotope analysis. Limnol. Oceanogr. Methods 3:408–418. doi: 10.4319/lom.2005.3.408

Kirschke S, Bousquet P, Ciais P, Saunois M, Canadell JG, Dlugokencky EJ, et al. 2013. Three decades of global methane sources and sinks. Nat. Geosci. 6:813–823. doi: 10.1038/ngeo1955

Lopez M, Sherwood OA, Dlugokencky EJ, Kessler R, Giroux L, Worthy DEJ. 2017. Isotopic signatures of anthropogenic CH4 sources in Alberta, Canada. Atmos. Environ. 164:280–288. doi: 10.1016/j.atmosenv.2017.06.021

Lowry D, Holmes CW, Rata ND, O'Brien P, Nisbet EG. 2001. London methane emissions: Use of diurnal changes in concentration and δ13C to identify urban sources and verify inventories. J. Geophys. Res. Atmospheres 106:7427–7448. doi: 10.1029/2000JD900601

Maasakkers JD, Jacob DJ, Sulprizio MP, Scarpelli TR, Nesser H, Sheng J-X, et al. 2019. Global distribution of methane emissions, emission trends, and OH concentrations and trends inferred from an inversion of GOSAT satellite data for 2010–2015. Atmospheric Chem. Phys. 19:7859–7881. doi: 10.5194/acp-19-7859-2019

Maazallahi H, Fernandez JM, Menoud M, Zavala-Araiza D, Weller ZD, Schwietzke S, et al. 2020. Methane mapping, emission quantification, and attribution in two European cities: Utrecht (NL) and Hamburg (DE). Atmospheric Chem. Phys. 20:14717–14740. doi: 10.5194/acp-20-14717-2020

Melchert JO, Stolz A, Dewald A, Gierga M, Wischhöfer P, Rethemeyer J. 2019. Exploring sample size limits of AMS gas ion source ^{14}C analysis at Cologneams. Radiocarbon 61: 1785–1793. doi: 10.1017/RDC.2019.143

Myhre G, Shindell D, Bréon F-M, Collins W, Fuglestvedt J, Huang J, Koch D, Lamarque J-F, Lee D, Mendoza B. et al. 2013. Anthropogenic and Natural Radiative Forcing. Climate Change 2013: The Physical Science Basis. Contribution of Working Group I to the Fifth Assessment Report of the Intergovernmental Panel on Climate Change 9781107057:659–740. doi: 10.1017/CBO9781107415324.018

Pack MA, Xu X, Lupascu M, Kessler JD, Czimczik CI. 2015. A rapid method for preparing low volume CH_4 and CO_2 gas samples for ^{14}C AMS analysis. Org. Geochem. 78:89–98. doi: 10.1016/j.orggeochem.2014.10.010

Palonen V, Uusitalo J, Seppälä E, Oinonen M. 2017. A portable methane sampling system for radiocarbon-based bioportion measurements and environmental CH_4 sourcing studies. Rev. Sci. Instrum. 88, 075102. doi: 10.1063/1.4993920

Petrenko VV, Smith AM, Brailsford G, Riedel K, Hua Q, Lowe D, et al. 2008. A new method for analyzing ^{14}C of methane in ancient air extracted from glacial ice. Radiocarbon 50: 53–73. doi: 10.1017/S0033822200043368

Pohlman JW, Kaneko M, Heuer VB, Coffin RB, Whiticar M. 2009. Methane sources and production in the northern Cascadia margin gas hydrate system. Earth Planet. Sci. Lett. 287: 504–512. doi: 10.1016/j.epsl.2009.08.037

https://doi.org/10.1017/RDC.2023.109 Published online by Cambridge University Press

Rethemeyer J, Fülöp R-H, Höfle S, Wacker L, Heinze S, Hajdas I, Patt U, König S, Stapper B, Dewald A. 2013. Status report on sample preparation facilities for 14C analysis at the new CologneAMS center. Nucl. Instrum. Methods Phys. Res. Sect. B 294:168–172. doi: 10.1016/j.nimb.2012.02.012

Ruff M, Szidat S, Gäggeler HW, Suter M, Synal H-A, Wacker L. 2010. Gaseous radiocarbon measurements of small samples. Nucl. Instrum. Methods Phys. Res. Sect. B 268:790–794. doi: 10.1016/j.nimb.2009.10.032

Saunois M, Jackson RB, Bousquet P, Poulter B, Canadell JG. 2016. The growing role of methane in anthropogenic climate change. Environmental Research Letters 11(12):120207. doi: 10.1088/1748-9326/11/12/120207

Saunois M, Stavert AR, Poulter B, Bousquet P, Canadell JG, Jackson RB, et al. 2020. The Global Methane Budget 2000–2017. Earth Syst. Sci. Data 12:1561–1623. doi: 10.5194/essd-12-1561-2020.

Sparrow KJ, Kessler JD. 2017. Efficient collection and preparation of methane from low concentration waters for natural abundance radiocarbon analysis. Limnol. Oceanogr. Methods 15:601–617. doi: 10.1002/lom3.10184

Townsend-Small A, Tyler SC, Pataki DE, Xu X, Christensen LE. 2012. Isotopic measurements of atmospheric methane in Los Angeles, California, USA: Influence of "fugitive" fossil fuel emissions. Journal of Geophysical Research: Atmospheres 117(D7). doi: 10.1029/2011JD016826

Townsend-Small A, Botner EC, Jimenez KL, Schroeder JR, Blake NJ, Meinardi, S, et al. 2016. Using stable isotopes of hydrogen to quantify biogenic and thermogenic atmospheric methane sources: A case study from the Colorado Front Range. Geophys. Res. Lett. 43: 11,462–11,471. doi: 10.1002/2016GL071438

Turner AJ, Frankenberg C, Wennberg PO, Jacob DJ. 2017. Ambiguity in the causes for decadal trends in atmospheric methane and hydroxyl. Proc. Natl. Acad. Sci. 114:5367–5372. doi: 10.1073/pnas.1616020114

Wotte A, Wordell-Dietrich P, Wacker L, Don A, Rethemeyer J. 2017. $^{14}CO_2$ processing using an improved and robust molecular sieve cartridge. Nucl. Instrum. Methods Phys. Res. Sect. B 400:65–73. doi: 10.1016/j.nimb.2017.04.019

Zazzeri G, Xu X, Graven H. 2021. Efficient sampling of atmospheric methane for radiocarbon analysis and quantification of fossil methane. Environ. Sci. Technol. 55:8535–8541. doi: 10.1021/acs.est.0c03300